Autocorrelation and Coherence Time of Interference in Poisson Networks

Udo Schilcher, Jorge F. Schmidt, Mahin K. Atiq, and Christian Bettstetter, *Senior Member, IEEE*

Abstract—This article takes an analytical approach to investigate the temporal dynamics of interference in wireless networks. We propose a framework to calculate the autocorrelation of interference in Poisson networks and derive closed-form expressions for the case of Nakagami fading. The framework takes three correlation sources into account: the location of interferers, the wireless channel, and the data traffic. We introduce the interference coherence time—in analogy to the well-established channel coherence time—and show how its basic qualitative behavior depends on the source of correlation. The insights gained can be useful in the design of medium access control and retransmission protocols.

Index Terms—Interference, autocorrelation, coherence time, Poisson point process, retransmission protocols

1 Introduction

In mobile communication and computer networks, the way how the received signal power varies over time has significant impact on the system design and performance. This dynamics can be quantified by the *autocorrelation* of the power signal, which describes how similar two values separated by a time lag τ are expected to be, thus indicating how fast the reception power typically changes over time. The time it takes the autocorrelation to reach a low value is called *coherence time* [1]. It basically tells us how long we need to wait in order to obtain an uncorrelated value with high probability. Knowledge of this dynamics is essential to the design of channel coding, interleaving, medium access, and retransmission protocols, to name a few examples.

Expressions for the autocorrelation function and coherence time are known for different types of fading channels but always *without consideration of interference*—they basically describe the signal received from a single source. Interference is typically modeled only by its average value or distribution without consideration of its dynamics. There is some recent work on interference dynamics (see [2], [3], [4], [5], [6]), but general expressions for the autocorrelation and coherence time are largely missing. Such expressions would serve a similar purpose as the ones for channel correlation. They would give answers to questions such as: How rapidly does interference change? Which parameters influence this correlation? How long should a retransmission protocol wait before sending again? Besides these basic examples, interference correlation could also be used for interference prediction [7].

The reason why the autocorrelation of interference is still unknown is that almost all work on interference dynamics considers the node locations as the sole source of correlation and ignores other relevant sources of correlation. This shortcoming leads to an autocorrelation that is constant over τ [8] not being useful for system design.

The article at hand investigates the autocorrelation of interference considering the channel and data traffic as two additional correlation sources besides the node locations. This analysis is performed with interferers distributed by a homogeneous Poisson point process and communicating over a wireless fading channel. Random access is performed without carrier sensing. Expressions are derived for an arbitrary time lag τ, thereby generalizing our previous work on interference autocorrelation in consecutive time slots ($\tau = 1$) [9]. The autocorrelation is also called *correlation* in the following.

Our contributions are as follows:

- *Framework for the calculation of interference correlation*. We present a mathematical expression of general validity for the temporal correlation of interference. It allows us to combine different correlation sources and modeling assumptions in a versatile and modular manner. In contrast to our previous work [9], it is no longer necessary to address all possible combinations of correlation sources individually. Furthermore, it is now possible to calculate the correlation for different channel and traffic models by substituting the correlation of these models into the general expression. Also mobile nodes can be considered.
- *Expressions for interference correlation*. We are the first to derive expressions for the correlation of interference in Poisson networks with Nakagami block fading and

- *U. Schilcher is with the Institute of Networked and Embedded Systems, University of Klagenfurt, Lakeside B02a, Klagenfurt am Wörthersee 9020, Austria, and also with the Lakeside Labs GmbH, Lakeside B04b, Klagenfurt am Wörthersee 9020, Austria. E-mail: udo.schilcher@aau.at.*
- *J. F. Schmidt is with the Lakeside Labs GmbH, Lakeside B04b, Klagenfurt am Wörthersee 9020, Austria. E-mail: schmidt@lakeside-labs.com.*
- *M. K. Atiq and C. Bettstetter are with the Institute of Networked and Embedded Systems, University of Klagenfurt, Lakeside B02a, Klagenfurt am Wörthersee 9020, Austria. E-mail: {mahin.atiq, christian.bettstetter}@aau.at.*

Manuscript received 8 May 2018; revised 1 Mar. 2019; accepted 11 Apr. 2019. Date of publication 23 Apr. 2019; date of current version 3 June 2020. (Corresponding author: Udo Schilcher.)
Digital Object Identifier no. 10.1109/TMC.2019.2912373

with Rayleigh fading according to Clarke's model considering three key sources of correlation. These expressions shed light on the interference dynamics beyond existing results and may lead to new techniques to exploit the temporal features of interference.

- *Coherence time of interference*. We introduce the interference coherence time and are able to derive closed-form expressions in some cases. Results could be used by a retransmission protocol to compute the waiting time for a retransmission.
- *Insights on interference dynamics*. The numerical evaluations of correlation and coherence time lead to some insights: First, the correlation caused by node locations will decrease over τ only if there are *mobile* nodes, and it is non-negative at all times. If the channel or traffic is the cause of correlation, negative correlation can occur as well. The latter is interesting for system design since it is unlikely that two time slots separated by a period with negative correlation both experience high interference. Second, a comparison of Nakagami block fading [10] and Clarke's model [11] suggests that the qualitative behavior of their correlation is similar and, in particular, the differences in their coherence times are negligible. Third, the basic qualitative behavior of the coherence time is fundamentally different for different sources of correlation: depending on the dominant source, there is either a monotonic increase or decrease with increasing traffic.

The article is organized as follows: Section 2 discusses related work. Section 3 introduces the modeling assumptions. Section 4 provides two expressions of general validity for the temporal correlation of interference. Section 5 derives sub-expressions and analyzes the interference correlation for all sources of correlation and their combinations. Section 6 derives and analyzes the interference coherence time. Finally, Section 7 concludes.

2 Related Work

There are results on the temporal correlation of interference in Poisson networks (see [6], [8], [9], [12], [13], [14]) and for the stochastic dependency of interference, typically expressed as the joint outage probability of multiple transmissions (see [4], [5], [6], [15], [16], [17], [18], [19]). In all these publications, however, the node locations are the sole source of correlation and mobility is not considered. Thus, the correlation or outage probability is independent of the time instants of transmissions, and neither temporal progression of the correlation nor coherence time is analyzed.

An exception to this limitation is the work by Gong and Haenggi (see [20], [21]). They still consider the node locations as the sole source of correlation but model mobile nodes. The mobility causes a decrease of the correlation for increasing τ. The analysis is performed for different stochastic mobility models, including Brownian motion (which is also used in the article at hand). However, the dependence of the correlation on τ is not comprehensively analyzed and no notion of coherence time is discussed.

Our previous work on interference correlation [9] takes the node locations, channel, and traffic into account. It addresses all 27 possible combinations of these sources but gives expressions only for consecutive time slots ($\tau = 1$), which is only a special case and provides no insight into the coherence time.

3 System Model

3.1 Node Location and Traffic

We consider a Poisson network: a wireless network consisting of nodes randomly located in a plane according to a Poisson point process (PPP) Φ on $\mathbb{R}^2$. The medium access opportunities are arranged into time slots. In each slot, every idle node decides independently from other nodes whether or not to start a new transmission. The duration of this transmission is $d \in \mathbb{N}$ time slots (message length), which is constant for all nodes and over time. We consider the case where on average a fraction p of all nodes in Φ starts a new transmission in each slot. Since only idle nodes start new transmissions, they adopt a sending probability of $\frac{p}{1-p(d-1)}$. Let q denote the probability that a node stays idle, i.e., $q = 1 - \frac{p}{1-p(d-1)}$ and S_t denote the set of all sending nodes at time t. The expected fraction of nodes sending in a given time slot t is thus $\mu = |S_t| = p\,d$, which we refer to as the traffic intensity (note that $\mu = p\,d \leq 1$). This traffic model is simple and aids mathematical analysis. We are well aware of more sophisticated models, such as [22] and [23], but stick to the simple model partly to get closed-form results and partly to avoid a wide range of details and parameters of the traffic model making the results very specific with regard to networking scenarios.

3.2 Node Mobility

Both static and mobile nodes are investigated. For mobile nodes, we let v denote the velocity of all nodes and consider two mobility models: linear mobility and time-discrete Brownian motion. The linear mobility model assumes the location of each node x at times t and $t+\tau$ to change in a random direction with $|x_t - x_{t+\tau}| = v\tau$, i.e., the distance increases linearly with time, all nodes have the same constant velocity. This can be considered to be a reasonable model for time spans covering the duration of a few time slots, as the direction of movement and velocity does not change significantly within the timescale of a slot in a practical system.

The location of a node x with Brownian motion at time $t+\tau$ is $x_{t+\tau} = x_t + v\omega_\tau$ [20], [21]. Here, ω_τ is given by

$$\omega_\tau = \sum_{t=1}^{\tau} \omega_t \overset{d}{=} \sqrt{\tau}\,\omega_0, \tag{1}$$

where $\overset{d}{=}$ denotes the equality in distribution and ω_t are i.i.d. two-dimensional Gaussian random variables $\omega_t \sim N(\vec{0}, \Sigma)$ with covariance matrix

$$\Sigma = \begin{pmatrix} 0 & \sqrt{\frac{2}{\pi}} \\ \sqrt{\frac{2}{\pi}} & 0 \end{pmatrix}. \tag{2}$$

Remark. The homogeneity of the PPP describing the node locations is not altered by these two mobility models. At any time t, the location of nodes forms a PPP with intensity λ. Note that this preservation of homogeneity is not provided by many other mobility models (e.g., the

random waypoint model lets nodes asymptotically concentrate in the center of the deployment area [24]).

3.3 Wireless Channel

The wireless channel is modeled by a distance dependent path loss and multipath fading accounting for reflections, diffraction, and other small-scale propagation effects. The signal power at a receiver x from an active sender y, with $x, y \in \mathbb{R}^2$, is

$$p_{\mathrm{RX}} = \kappa\, h_t^2\, \ell_{xy}. \tag{3}$$

In this equation, κ is the sending power of y, which we consider to be the same for all nodes in the network. The term $\ell_{xy} = \ell(\|y - x\|)$ denotes a non-singular distance dependent path loss, for which we adopt

$$\ell(\|y - x\|) = \min(1, \|y - x\|^{-\alpha}), \tag{4}$$

with a path loss exponent $\alpha > 2$. Let $\ell_x = \ell(\|x - o\|) = \ell(\|x\|)$ be the path loss from a node x to the origin o.

Fading is modeled by the fading coefficient h_t^2 at time t (h_t is the signal envelope gain). We use two well-known fading models: Nakagami and Rayleigh fading. Using Nakagami-m fading, h_t^2 is gamma distributed according to $h_t^2 \sim \Gamma(m, m)$. This implies $\mathbb{E}\left[h_t^2\right] = 1$ and $\mathbb{E}\left[h_t^4\right] = \frac{m+1}{m}$. The temporal aspect of Nakagami fading is modeled as block fading [9], where the channel is assumed to remain constant over a duration of $c \in \mathbb{N}$ time slots after which it changes to an independent state, i.e., a random experiment is carried out independently of the previous channel state to establish the new channel state. This model for the temporal behavior is of widespread use. It matches well practical systems where the signal timing is usually designed to approximately meet this condition for easing the channel state acquisition and equalization tasks.

Using Rayleigh fading, h_t^2 is exponentially distributed with mean $\mathbb{E}\left[h_t^2\right] = 1$ and second moment $\mathbb{E}\left[h_t^4\right] = 2$. The temporal evolution follows Clarke's model, where the channel power autocorrelation is approximately given by (see Appendix B in [11])

$$\rho\left[h_{t_1}^2, h_{t_2}^2\right] \approx J_0^2(2\pi f_D \tau), \tag{5}$$

where $\tau = t_2 - t_1$, $J_0(x)$ is the Bessel function of zeroth order, and $f_D = 2 f_0 \frac{v}{\nu}$ denotes the Doppler spread, where f_0 is the carrier frequency, v is the relative velocity, and ν is the speed of light.

The channel coherence time is the time span until the correlation falls below a small fraction of its initial value, e.g., the smallest τ such that $\rho\left[h_t^2, h_{t+\tau}^2\right] = 0.05\rho\left[h_t^2, h_t^2\right]$. For Clarke's model, it can be calculated by [25]

$$c = \frac{J_0^{-1}(\sqrt{0.05})}{2\pi f_D}. \tag{6}$$

3.4 Interference

Interference at time t is measured at the origin o of $\mathbb{R}^2$, which is equal to the interference experienced by a typical node of the network due to Slivnyak's theorem. Its power is the sum of the signal powers received from all sending nodes in the network (besides the intended signal from a specific sender, which is not considered in this work):

$$I_t = \sum_{x \in \Phi} \kappa\, h_t^2\, \ell_x\, \gamma_t, \tag{7}$$

where γ_t is a Bernoulli random variable indicating whether node x is sending ($\gamma_t = 1$) at time t or not ($\gamma_t = 0$).

3.5 Classification of Correlation Sources

We consider three sources of correlation of interference: node locations, wireless channel (i.e., correlated fading), and traffic. For each of them, there are three possible options, denoted by a triplet $(i, j, k) \in \{0, 1, 2\}^3$:

- They are constant or the correlation is not considered (denoted by 0).
- They are random but uncorrelated (denoted by 1).
- They are random and correlated (denoted by 2).

This leads to 27 cases that have been introduced and analyzed with respect to temporal correlation of interference with $\tau = 1$ in [9].

4 Interference Correlation Derivation

We now derive general expressions for the correlation of interference. Interference correlation is measured in terms of Pearson's correlation coefficient:

$$\rho(\tau) = \rho\left[I_{t_1}, I_{t_2}\right] = \frac{\mathrm{cov}\left[I_{t_1}, I_{t_2}\right]}{\sqrt{\mathrm{var}\left[I_{t_1}\right]\mathrm{var}\left[I_{t_2}\right]}} = \frac{\mathrm{cov}\left[I_{t_1}, I_{t_2}\right]}{\mathrm{var}[I]}, \tag{8}$$

with the covariance $\mathrm{cov}\left[I_{t_1}, I_{t_2}\right] = \mathbb{E}\left[I_{t_1} I_{t_2}\right] - \mathbb{E}\left[I_{t_1}\right]\mathbb{E}\left[I_{t_1}\right]$ of interference at time instants t_1 and t_2, and its variance $\mathrm{var}[I] = \mathrm{var}\left[I_{t_1}\right] = \mathrm{var}\left[I_{t_2}\right]$, which is constant over time due to the stationarity of the processes involved. The time lag from t_1 to t_2 is $\tau = t_2 - t_1$.

We distinguish between random locations (cases $(2, j, k)$) leading to interference correlation and known locations (cases $(0, j, k)$) not contributing to interference correlation.

4.1 Random Node Locations

Theorem 1 (Correlation for cases $(2, j, k)$). *The temporal correlation of interference between time instants t_1 and t_2 considering the node locations as a source of correlation is*

$$\rho(\tau) = \frac{\mathbb{E}\left[h_{t_1}^2 h_{t_2}^2\right]\mathbb{E}\left[\gamma_{t_1}\gamma_{t_2}\right]}{\mu\, \mathbb{E}[h_t^4]} \cdot \frac{\int_{\mathbb{R}^2} \ell_x\, \mathbb{E}[\ell(\|x + v\omega_\tau\|)]\, \mathrm{d}x}{\int_{\mathbb{R}^2} \ell_x^2\, \mathrm{d}x}. \tag{9}$$

Proof. The expected value of interference is

$$\begin{aligned} \mathbb{E}[I] &= \mathbb{E}_{\Phi,h,\gamma} \sum_{x \in \Phi} h_x^2\, \ell_x \gamma_t \\ &= \mathbb{E}_\Phi \sum_{x \in \Phi} \mathbb{E}_h[h_t^2]\, \ell_x\ \mathbb{E}_\gamma[\gamma_t] \\ &\overset{(a)}{=} dp\, \lambda \int_{\mathbb{R}^2} \ell_x\, \mathrm{d}x \\ &= \mu\, \lambda\, \frac{\alpha\pi}{\alpha - 2}, \end{aligned} \tag{10}$$

where (a) holds due to Campbell's theorem [4], $\mathbb{E}\left[h_t^2\right] = 1$ for all $x \in \Phi$ and $t \in \mathbb{N}$, and $\mathbb{E}[\gamma_t] = \mu = dp$. The indices for the expectation operator $\mathbb{E}$ indicate the random variables involved and will be omitted in the future. Aiming for the covariance, we calculate

$$\begin{aligned}\mathbb{E}\big[I_{t_1} I_{t_2}\big] &= \mathbb{E}\left[\sum_{x\in\Phi} h_{t_1}^2\, \ell_x \gamma_{t_1} \sum_{y\in\Phi} \tilde{h}_{t_2}^2 \ell(\|y+v\omega_\tau\|)\tilde{\gamma}_{t_2}\right] \\ &= \mathbb{E}\left[\sum_{x\in\Phi} h_{t_1}^2 h_{t_2}^2 \ell_x\, \ell(\|x+v\omega_\tau\|)\gamma_{t_1}\gamma_{t_2}\right] \\ &\quad + \mathbb{E}\left[\sum_{\substack{x,y\in\Phi\\ x\neq y}} h_{t_1}^2 \tilde{h}_{t_2}^2 \ell_x\, \ell(\|y+v\omega_\tau\|)\gamma_{t_1}\tilde{\gamma}_{t_2}\right],\end{aligned} \tag{11}$$

where we introduce $\tilde{h}_t$ and $\tilde{\gamma}_t$ to denote the fading coefficient and sending indicator of node y at time t, respectively. The first of the two expected values of (11) is

$$\begin{aligned}&\mathbb{E}\left[\sum_{x\in\Phi} h_{t_1}^2 h_{t_2}^2 \ell_x\, \ell(\|x+v\omega_\tau\|)\gamma_{t_1}\gamma_{t_2}\right] \\ &= \mathbb{E}\left[\sum_{x\in\Phi} \mathbb{E}\Big[h_{t_1}^2 h_{t_2}^2\Big] \ell_x\, \mathbb{E}[\ell(\|x+v\omega_\tau\|)]\mathbb{E}\Big[\gamma_{t_1}\gamma_{t_2}\Big]\right] \\ &= \mathbb{E}\Big[h_{t_1}^2 h_{t_2}^2\Big]\, \mathbb{E}\Big[\gamma_{t_1}\gamma_{t_2}\Big]\, \lambda \int_{\mathbb{R}^2} \ell_x\, \mathbb{E}[\ell(\|x+v\omega_\tau\|)]\mathrm{d}x,\end{aligned} \tag{12}$$

and the second gives

$$\mathbb{E}\left[\sum_{\substack{x,y\in\Phi\\ x\neq y}} h_{t_1}^2 \tilde{h}_{t_2}^2 \ell_x\, \mathbb{E}[\ell(\|y+v\omega_\tau\|)]\gamma_{t_1}\tilde{\gamma}_{t_2}\right] = \mathbb{E}[I]^2 \tag{13}$$

due to the independence of node locations, channel, and traffic in case of $x \neq y$. Hence, the covariance is

$$\begin{aligned}\mathrm{cov}\big[I_{t_1}, I_{t_2}\big] &= \mathbb{E}\big[I_{t_1} I_{t_2}\big] - \mathbb{E}\big[I_{t_1}\big]\mathbb{E}\big[I_{t_2}\big] \\ &= \mathbb{E}\Big[h_{t_1}^2 h_{t_2}^2\Big]\, \mathbb{E}\Big[\gamma_{t_1}\gamma_{t_2}\Big]\, \lambda \int_{\mathbb{R}^2} \ell_x\, \mathbb{E}[\ell(\|x+v\omega_\tau\|)]\, \mathrm{d}x.\end{aligned} \tag{14}$$

The values of $\mathbb{E}[h_{t_1}^2 h_{t_2}^2]$ and $\mathbb{E}[\gamma_{t_1}\gamma_{t_2}]$ characterize the contributions of the channel and the traffic to the interference correlation. They depend on the values of j and k of the case $(2, j, k)$ under consideration.

The variance is obtained by setting $t_1 = t_2$, yielding

$$\mathrm{var}[I] = \mathrm{cov}[I, I] = \mu\, \mathbb{E}\big[h_t^4\big]\, \lambda \int_{\mathbb{R}^2} \ell_x^2\, \mathrm{d}x. \tag{15}$$

Dividing (14) by (15) yields the result. □

Remark. This result holds for any mobility model for which the node locations form a stationary PPP in each time slot t. The PPPs in different time slots do not have to be stochastically independent.

Corollary 1 (Correlation for cases $(2, j, k)$ without mobility). *The temporal correlation of interference between t_1 and t_2 considering the node locations as sources of interference correlation and having no mobility is*

$$\rho(\tau) = \frac{\mathbb{E}\Big[h_{t_1}^2 h_{t_2}^2\Big]\, \mathbb{E}\Big[\gamma_{t_1}\gamma_{t_2}\Big]}{\mu\, \mathbb{E}[h_t^4]}. \tag{16}$$

Proof. Substituting $v = 0$ into (9) yields the result. □

4.2 Known Node Locations

Theorem 2 (Correlation for cases $(0, j, k)$). *The temporal correlation of interference between t_1 and t_2 if neglecting the node locations as sources of correlation is*

$$\rho(\tau) = \frac{\mathbb{E}\Big[h_{t_1}^2 h_{t_2}^2\Big]\, \mathbb{E}\Big[\gamma_{t_1}\gamma_{t_2}\Big] - \mu^2}{\mu\, \mathbb{E}[h_t^4] - \mu^2}. \tag{17}$$

Proof. The covariance of interference is

$$\begin{aligned}\mathrm{cov}\big[I_{t_1}, I_{t_2}\big] &= \mathbb{E}\left[\sum_{x\in\Phi}\sum_{y\in\Phi} \mathrm{cov}\Big[h_{t_1}^2\, \ell_x\gamma_{t_1}, \tilde{h}_{t_2}^2\, \ell_y\, \tilde{\gamma}_{t_2}\Big]\right] \\ &= \mathbb{E}\left[\sum_{x\in\Phi} \mathrm{cov}\Big[h_{t_1}^2\, \ell_x\gamma_{t_1}, h_{t_2}^2\, \ell_x\gamma_{t_2}\Big]\right] \\ &\quad + \mathbb{E}\left[\sum_{\substack{x,y\in\Phi\\ x\neq y}} \mathrm{cov}\Big[h_{t_1}^2\, \ell_x\gamma_{t_1}, \tilde{h}_{t_2}^2\, \ell_y\, \tilde{\gamma}_{t_2}\Big]\right].\end{aligned} \tag{18}$$

The covariance in the second sum is always zero as the arguments are stochastically independent. The covariance in the first sum yields

$$\begin{aligned}&\mathbb{E}\left[\sum_{x\in\Phi} \mathrm{cov}\Big[h_{t_1}^2\, \ell_x\gamma_{t_1}, h_{t_2}^2\, \ell_x\gamma_{t_2}\Big]\right] \\ &\overset{(a)}{=} \mathbb{E}\left[\sum_{x\in\Phi} \mathbb{E}\Big[h_{t_1}^2 h_{t_2}^2\Big]\, \ell_x^2\, \mathbb{E}\Big[\gamma_{t_1}\gamma_{t_2}\Big] - \big(\mathbb{E}\big[h_t^2\big]\, \ell_x\, \mathbb{E}[\gamma_t]\big)^2\right] \\ &\overset{(b)}{=} \Big(\mathbb{E}\Big[h_{t_1}^2 h_{t_2}^2\Big]\, \mathbb{E}\Big[\gamma_{t_1}\gamma_{t_2}\Big] - \mu^2\Big)\, \lambda \int_{\mathbb{R}^2} \ell_x^2\, \mathrm{d}x,\end{aligned} \tag{19}$$

where in (a) we calculate the covariance with $\mathrm{cov}[X, Y] = \mathbb{E}[XY] - \mathbb{E}[X]\mathbb{E}[Y]$ and in (b) we substitute $\mathbb{E}\big[h_t^2\big] = 1$ and $\mathbb{E}[\gamma_t] = \mu$. The variance is given by

$$\mathrm{var}[I] = \mathrm{cov}[I, I] = \big(\mu\, \mathbb{E}\big[h_t^4\big] - \mu^2\big)\, \lambda \int_{\mathbb{R}^2} \ell_x^2\, \mathrm{d}x. \tag{20}$$

Dividing (19) by (20) yields the result. □

Remarks.

- Theorem 2 does not include mobility, since the node locations are not considered.
- The correlation is $\rho(\tau) \equiv 0$ for all cases $(1, j, k)$.
- Theorems 1 and 2 are generally valid, independent of the channel and traffic models used. In particular, the correlation is influenced by these models only via $\mathbb{E}[h_{t_1}^2 h_{t_2}^2]$ in case of channel and via $\mathbb{E}[\gamma_{t_1}\gamma_{t_2}]$ and μ in case of traffic. Hence, any model can be incorporated into this framework by substituting expressions for these expected values accordingly.

5 Interference Correlation Analysis

Using the general expressions derived, we can now analyze the interference correlation for the three sources of correlation. We start by treating these sources individually and afterward study some combinations. A summary of some

TABLE 1
Correlation and Coherence Time of Interference for Nakagami Block Fading without Mobility

Locations i	Channel j	Traffic k	Correlation $\rho(\tau)$	Coherence time τ_c
0	0	0	undefined	undefined
0	0	1	0	1
0	0	2	$\frac{q^\tau+\mu-1}{\mu}$ for $\tau < d$	$\frac{\log(1-\mu)}{\log q}$
0	1	0	0	1
0	1	1	0	1
0	1	2	$\frac{m(\mu-1)(q^\tau+\mu-1)}{\mu(m(\mu-1)-1)}$ for $\tau < d$	$\frac{\log(1-\mu)}{\log q}$
0	2	0	$1-\frac{\tau}{c}$ for $\tau \leq c$	c
0	2	1	$\frac{p(c-\tau)}{c(1+m-mp)}$ for $\tau < c$	c
0	2	2	$\frac{(q^\tau(\mu-1)-2\mu+1)(\tau-c(m+1))-cm\mu^2}{c\mu(1+m-m\mu)}$ for $\tau < \min(c,d)$	–
1	0, 1, or 2	0, 1, or 2	0	1
2	0	0	1	∞
2	0	1	p	∞
2	1	0	$1/2$	∞
2	1	1	$p/2$	∞
2	0,1	2	$\frac{q^\tau(1-\mu)+2\mu-1}{\mathbb{E}[h^4]\mu}$ for $\tau < d$	–
2	2	0	$1-\frac{\tau}{c(m+1)}$ for $\tau < c$	–
2	2	1	$p\left(1-\frac{\tau}{c(m+1)}\right)$ for $\tau < c$	–
2	2	2	$\frac{(q^\tau(\mu-1)-2\mu+1)(\tau-c(m+1))}{c\mu(m+1)}$ for $\tau < \min(c,d)$	–

Coherence time expressions must be rounded to the next higher integer.

results is given in Table 1 for cases without mobility.[1] Substituting $\tau = 1$ and $m = 1$ leads to the correlation results of [9, Table 1].[2]

All plots in this section have been compared to simulation results, which show a good match. We refrain from plotting the simulation results as they would crowd the figures without providing any additional insights.

5.1 Correlation by Node Locations

The locations of the interfering nodes introduce a correlation that can be interpreted in the following way: If a receiver has close-by interferers, it is more likely to be disturbed during the reception of a message as if no interferers are close. Without mobility, this correlation is independent of τ, i.e., $\rho(\tau_1) = \rho(\tau_2)$ for all $\tau_1, \tau_2 \in \mathbb{Z}$.

We investigate the relation between outage probability and the interference correlation with $\tau = 1$. For this purpose, we consider a communication link between a receiver at the origin o and a sender one length unit away from the receiver. This link is in outage if the signal-to-interference ratio (SIR) is below 1, i.e.,

$$\frac{h^2}{\sum_{x\in\Phi} h_x^2\, \ell_x\, \gamma_x} < 1, \tag{21}$$

where h^2 is the channel state between sender and receiver, and the denominator is defined in (7). We are particularly interested in a link being n times in outage

$$\begin{aligned}
&\mathbb{P}\left[\mathrm{SIR}_1 < 1, \ldots, \mathrm{SIR}_n < 1\right] \\
&\quad = \mathbb{E}\left[\exp\left(-\sum_{x\in\Phi} h_x^2 \left\|x\right\|^{-\alpha} \mathbf{1}_x\right)^n\right] \\
&\quad = \exp\left(-\lambda \int_{\mathbb{R}^2} 1 - \left(\frac{p}{1+\ell_x} + 1 - p\right)^n \mathrm{d}x\right),
\end{aligned} \tag{22}$$

where Rayleigh fading ($m = 1$) is assumed. Details of the derivation can be found in [26].

Fig. 1 shows the outage probabilities over varying interference correlation $\rho(1)$ while keeping the expected interference $\mathbb{E}[I]$ constant. The constant $\mathbb{E}[I]$ is achieved by setting $\lambda p = 10^{-4}$ and varying p to change the correlation. In this particular case, the correlation is $\rho(1) = \frac{p}{2}$. As can be seen in the plot, interference correlation does not affect the outage probability for $n = 1$ but has significant impact on outage if $n > 1$. In the high correlation regime, the outage probability is several orders of magnitude higher than for low outage. This probability approaches the probability of a single outage event for increasing $\rho(1)$. In the low correlation regime, the n outage events of a given link become almost independent, and in the limiting case $\rho(1) \to 0$ they become independent, i.e., $\lim_{\rho(1)\to 0} \mathbb{P}\left[\mathrm{SIR}_1 < 1, \ldots, \mathrm{SIR}_n < 1\right] = \left(\mathbb{P}\left[\mathrm{SIR} < 1\right]\right)^n$.

In case of mobility, the interference correlation decreases with increasing τ [21], depending on the velocity v and the type of mobility. Fig. 2 shows the correlation over τ for both linear mobility and Brownian motion. For the same v, the distance traveled in time τ is on average smaller with Brownian motion, and hence the correlation decreases slower with τ. In general, the decrease of correlation depends only on the distance traveled during τ or its distribution in case it is random (e.g., for Brownian motion).

1. Expressions in Table 1 hold for small time lags $\tau < c$ and $\tau < d$ and without mobility. The general expressions, valid for arbitrary τ and mobility, are too long for the table but are available in the text. Coherence time results are computed by solving $\rho(\tau) = 0$ for τ, where some cases can only be solved numerically (marked as '–').

2. There is a difference in the cases $(i, 2, 1)$ and $(i, 2, 2)$ due to different modeling assumptions: the channel in this paper changes every cth slot; the channel in [9] changes c slots after a message start.

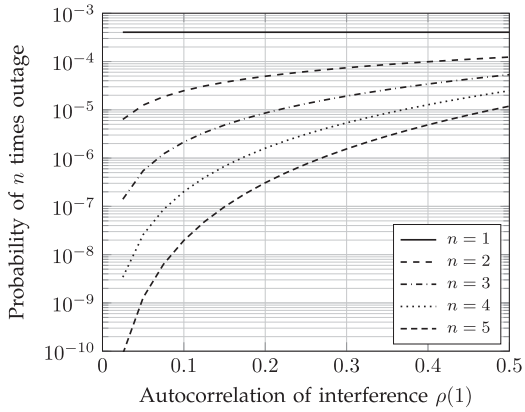

Fig. 1. Probability of a link being n times in outage over the interference correlation $\rho(1)$. The expected interference $\mathbb{E}[I]$ is constant by setting $\lambda p = 10^{-4}$. Other parameters are $\alpha = 4$ and $m = 1$.

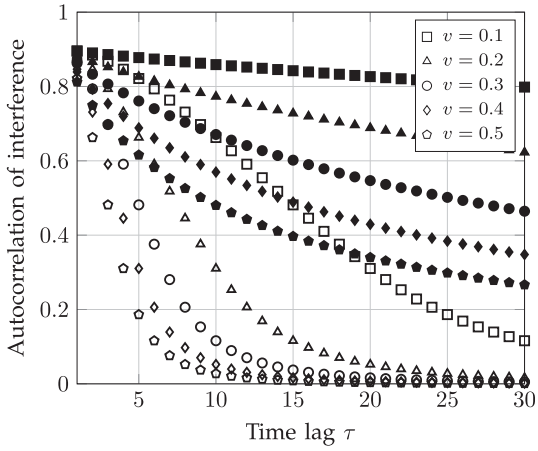

Fig. 2. Correlation for the case (2, 0, 1) for the linear mobility model (open marks) and for Brownian motion (filled marks) with different velocities v. The velocity is measured in meters per time slot and the sending probability is $p = 0.9$.

5.2 Correlation by Wireless Channel

5.2.1 Block Fading

The wireless channel is modeled as a block fading channel with length c slots. This means that the channel gain due to multipath propagation from a potential interferer stays unchanged for c slots and then changes to a stochastically independent value. This change is independent for each of the potential interferers. Hence, in each slot on average the channels of $\frac{1}{c}$ interferers change to a new state. This assumption introduces a correlation to the interference values of different slots for $c > 1$. In the expressions for interference correlation in Theorems 1 and 2, the effect of the channel of node x is covered by the term $\mathbb{E}[h_{t_1}^2 h_{t_2}^2]$. For Nakagami fading, this term depends on the fading parameter m, the channel block length c, and the time lag τ. It is given by

$$\mathbb{E}\left[h_{t_1}^2 h_{t_2}^2\right] = \begin{cases} \frac{m+1}{m} - \frac{\tau}{mc} & \text{for } \tau < c \\ 1 & \text{for } \tau \geq c. \end{cases} \tag{23}$$

In the special case of Rayleigh fading ($m = 1$), this term simplifies to $\mathbb{E}[h_{t_1}^2 h_{t_2}^2] = 2 - \frac{\tau}{c}$ for $\tau < c$.

Remark. If a node travels at least half the wavelength during a single slot, the channel can be assumed to be stochastically independent for consecutive slots, i.e., $c = 1$.

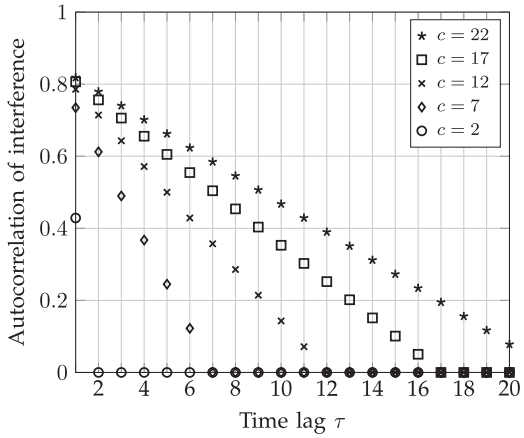

Fig. 3. Correlation for the case (0, 2, 1) for varying the channel block length c. The Nakagami fading parameter is $m = \frac{1}{2}$ and the sending probability is $p = 0.9$.

Under this assumption, fading does not contribute to interference correlation, and equations for cases $(i, 1, k)$ for $i, k \in \{0, 1, 2\}$ apply.

If the channel is the sole source of interference correlation, we are in a static case (0,2,1). A plot of interference correlation is shown in Fig. 3 for different values of the channel block length c. The correlation decreases linearly with τ and vanishes for all $\tau \geq c$. For a given τ, slower fading (higher values of c) implies a higher correlation. In the limit, for a constant channel, i.e., $c \to \infty$, we get

$$\lim_{c\to\infty} \rho(\tau) = \frac{p}{1 + m - mp}, \tag{24}$$

independent of τ.

5.2.2 Clarke's Model

The wireless channel is now modeled according to Clarke [11]. This implies Rayleigh fading, and hence the channel gain follows an exponential distribution. From the correlation of fading (5), it follows that

$$\mathbb{E}\left[h_{t_1}^2 h_{t_2}^2\right] \approx J_0^2(2\pi f_D \tau) + 1, \tag{25}$$

where $J_0(x)$ is the Bessel function of zeroth kind, and f_D denotes the Doppler frequency. This expression can be substituted into Theorem 2 to verify what happens if the channel is the sole source of correlation:

$$\rho(\tau) = \frac{\mathbb{E}\left[h_{t_1}^2 h_{t_2}^2\right] \mathbb{E}\left[\gamma_{t_1}\gamma_{t_2}\right] - \mu^2}{\mu\, \mathbb{E}[h_t^4] - \mu^2} = \frac{p\, J_0^2(2\pi f_D \tau)}{2 - p}, \tag{26}$$

which is shown in Fig. 4. If all nodes are transmitting ($p = 1$), we have the known result $\rho(\tau) = J_0^2(2\pi f_D \tau)$. For smaller p, the correlation takes smaller values, as expected. The interference coherence time is about three slots, which corresponds to the channel coherence time.

5.3 Correlation by Data Traffic

Correlated traffic is caused by $d > 1$, which impacts interference correlation via the expected value $\mathbb{E}[\gamma_{t_1}\, \gamma_{t_2}]$.

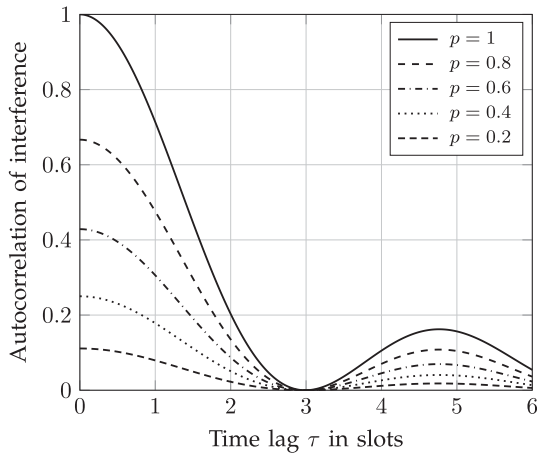

Fig. 4. Correlation of interference for the case (0, 2, 1) for varying the sending probability p. The Doppler frequency for Clarke's model is $f_D = 0.128$ leading to a channel coherence time of three time slots.

Lemma 1 (Traffic correlation). *The probability that a node sends in two given slots t_1 and t_2 is*

$$\mathbb{E}\left[\gamma_{t_1}\,\gamma_{t_2}\right] = \max\bigl(0, p\,(d-\tau)\bigr) + \frac{p^2}{1-p(d-1)} \sum_{i=0}^{\min(\tau-1,d-1)} \sum_{j=1}^{\min(\tau-i,d)} \sum_{k=0}^{\lfloor \frac{g}{d} \rfloor} \binom{g-kd+k}{k} q^{g-kd}(1-q)^k, \tag{27}$$

where $g = \tau - i - j$ and $q = 1 - \frac{p}{1-p(d-1)}$.

Proof. Let us assume that a certain node x sends in both slots t_1 and t_2. There are two possibilities: (I) a single message spans both slots or (II) two different messages are transmitted in these two slots. A message consists of d slots; we reference each of them by an index ranging over $1, 2, \ldots, d$. Let i denote the index of the message at t_1 and j the index at time t_2, and write the indices as tuples (i, j).

The probability $\mathbb{P}[\gamma^{\mathrm{I}}_{t_1,t_2}]$ that a single message spans over both t_1 and t_2 is given by

$$\mathbb{P}\left[\gamma^{\mathrm{I}}_{t_1,t_2}\right] = \begin{cases} p\,(d-\tau) & \text{for } d > \tau \\ 0 & \text{else.} \end{cases} \tag{28}$$

As shown in Fig. 6, this happens because in each slot a fraction of p nodes starts a transmission. For $d > \tau$, there are $d - \tau$ slots for which a message starting there would span both slots of interest. In this case, the indices (i, j) always differ by the time lag $j - i = \tau$. For $d \leq \tau$, the time period between t_1 and t_2 is larger than the message length, and hence, it is impossible that a single message spans both slots.

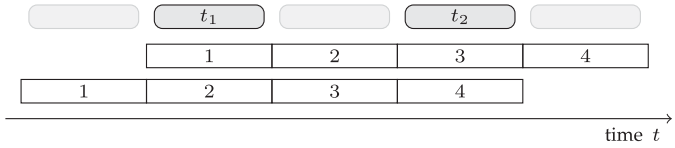

Fig. 6. An illustration of the slots in which transmissions start that each span over both slots t_1 and t_2. In the shown setup ($d = 4$ and $\tau = 2$), there are two possibilities: messages starting at t_1 having indices (1, 3) and messages starting at $t_1 - 1$ with indices (2, 4).

The probability $\mathbb{P}[\gamma^{\mathrm{II}}_{t_1,t_2}]$ of two different messages being transmitted at slots t_1 and t_2 is calculated by summing the probabilities of all possible indices (i, j) (see Fig. 5). The range of the index i is from $\max\bigl(1, d-(\tau-1)\bigr)$ to d, i.e., if $\tau \geq d$, we have $i = 1, \ldots, d$; in case $\tau < d$, the index i has to be big enough to avoid a single message spanning both slots t_1 and t_2. The range of the index j depends on the value of i, as the message covering slot t_2 must not overlap with the message covering t_1. Hence, j ranges from 1 to $\min\bigl(\tau - (d-i), d\bigr)$, i.e., if there is enough space between t_1 and t_2, j can go up to d; otherwise its maximum value is determined by the case where the two messages are transmitted directly one after another, as for the indices (1,1), (2,2), and (3.3) in Fig. 5.

In order to calculate the probability of the situation described by indices (i, j), we calculate the number of slots between the end of the message covering t_1 and the beginning of the message covering t_2 by

$$g = \tau - (d-i) - j. \tag{29}$$

These intermediate slots can be covered by additional messages if there is enough space, i.e., if $g \geq d$. The number k of messages fitting these intermediate slots is at most $k \leq \lfloor \frac{g}{d} \rfloor$ where $\lfloor x \rfloor$ denotes the biggest integer that is smaller than or equal to x. If k messages are present in the intermediate slots, there are $e = g - kd$ slots unoccupied. The probability of a message starting is $1 - q = \frac{p}{1-p(d-1)}$, as mentioned in Section 3, and the probability of an empty slot is $q = 1 - \frac{p}{1-p(d-1)}$. Therefore, the probability that t_1 and t_2 are occupied by different messages is

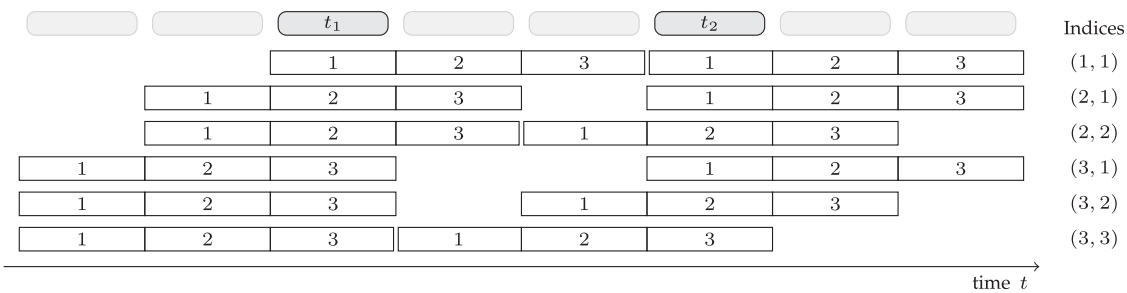

Fig. 5. An illustration of the potential starting slots of two messages covering t_1 and t_2. In the shown setup ($d = 3$ and $\tau = 3$), there are six possibilities, of which the indices are shown on the right hand side.

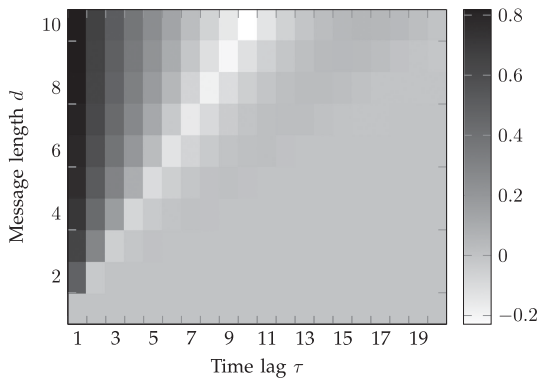

Fig. 7. Correlation for the case (0, 0, 2) for varying the message length d. The sending probability is $p = 0.05$.

$$\mathbb{P}\left[\gamma^{\mathrm{II}}_{t_1,t_2}\right] = \frac{p^2}{1-p(d-1)} \sum_{i=\max(1,d-(\tau-1))}^{d} \sum_{j=1}^{\min(\tau-(d-i),d)} \sum_{k=0}^{\lfloor \frac{q}{d} \rfloor} \binom{e+k}{k} \left(\frac{p}{1-p(d-1)}\right)^k \left(1-\frac{p}{1-p(d-1)}\right)^e. \tag{30}$$

Overall, we can sum the two probabilities calculated above to get the expected value $\mathbb{E}[\gamma_{t_1}\,\gamma_{t_2}] = \mathbb{P}[\gamma^{\mathrm{I}}_{t_1,t_2}] + \mathbb{P}[\gamma^{\mathrm{II}}_{t_1,t_2}]$. In (30) we substitute i by $i-d$ to get the result. □

Remark. In this lemma we assume that the message duration d is constant for all nodes. However, it is possible to modify our results to account for differences in message length. If we assume, for example, that each node uses its own randomly chosen message length d_x with d_x i.i.d., we could adopt our results by adjusting the expressions of $\mathbb{E}[\gamma_t]$ and $\mathbb{E}[\gamma_{t_1}\,\gamma_{t_2}]$ accordingly: The traffic intensity would change to $\mathbb{E}[\gamma_t] = \mu = p\,\mathbb{E}[d_x]$ throughout the article. Furthermore, the expression (27) in Lemma 1 represents the probability $\mathbb{E}[\gamma_{t_1}\,\gamma_{t_2}\,|\,d_x]$ and we would have to compute

$$\begin{aligned}\mathbb{E}\left[\gamma_{t_1}\,\gamma_{t_2}\right] &= \mathbb{E}_{d_x}\left[\mathbb{E}\left[\gamma_{t_1}\,\gamma_{t_2}\,|\,d_x\right]\right] \\ &= \sum_{i=0}^{\infty} \mathbb{E}\left[\gamma_{t_1}\,\gamma_{t_2}\,|\,d_x\right]\mathbb{P}\left[d_x = i\right],\end{aligned} \tag{31}$$

where $\mathbb{P}\left[d_x = i\right]$ is the probability that node x transmits with message length $d = i$.

Corollary 2 (Traffic correlation for $\tau \le d$). *If the lag τ is smaller than or equal to the message length, the result of Lemma 1 simplifies to*

$$\mathbb{E}\left[\gamma_{t_1}\,\gamma_{t_2}\right] = p\,(d-\tau) + p\,\frac{\tau(1-q)+q^{\tau+1}-q}{1-q}, \tag{32}$$

where $q = 1 - \frac{p}{1-p(d-1)}$.

Proof. If we consider the assumption $\tau \le d$ in (28), only the first case can occur. In (30), the upper bounds of the first two sums simplify to $\tau-1$ and $\tau-i$, respectively. In the third sum, the upper bound $\lfloor \frac{q}{d} \rfloor = 0$, and hence there is only one summand with $k=0$. Thus, we have $\binom{e+k}{k}\left(\frac{p}{1-p(d-1)}\right)^k = 1$, and overall we have

$$\mathbb{E}\left[\gamma_{t_1}\,\gamma_{t_2}\right] = p\,(d-\tau) + \frac{p^2}{1-p(d-1)} \sum_{i=0}^{\tau-1}\sum_{j=1}^{\tau-i}\left(1-\frac{p}{1-p(d-1)}\right)^{\tau-i-j}. \tag{33}$$

The inner sum of this expression is a geometric series (with the power being $0,\ldots,\tau-i-1$). After replacing the closed form result of the inner sum, the outer sum also results in a geometric series but with the first term ($i=0$) missing. Applying the sum expression of geometric series twice yields

$$\begin{aligned}\sum_{i=0}^{\tau-1}\sum_{j=1}^{\tau-i} q^{\tau-i-j} &= \sum_{i=0}^{\tau-1}\frac{1-q^{\tau-i}}{1-q} \\ &= \frac{\tau - \sum_{i=0}^{\tau-1} q^{\tau-i}}{1-q} \\ &= \frac{\tau - \frac{1-q^{\tau+1}}{1-q} + 1}{1-q},\end{aligned} \tag{34}$$

where the 1 is due to the sum starting at $i=1$ instead of 0. Applying some basic algebra leads to the result. □

We now investigate the temporal correlation of interference when the traffic is the sole source of correlation (case (0, 0, 2)). Fig. 7 shows a heat map of the interference correlation for different message lengths d. Correlation is highest for $\tau = 1$ and decreases until the lag matches the message length ($\tau = d$), where it is negative. For lags above d, it increases to reach a small positive value, from where a damped oscillating behavior is observed. The lag for which zero crossings exist depends, besides the message length, on the sending probability p: for higher p the correlation is in general smaller which implies that it reaches zero for smaller τ and it gets more negative at $\tau = d$.

A detailed study of the impact of p on correlation is presented in Fig. 8. Our first observation is that the traces can be separated into two groups: The influence of p is different for $d \le \tau$ than for $d > \tau$. For $d \le \tau$, the correlation is always negative if $d \bmod 2 = \tau \bmod 2$ or otherwise mostly positive; only for small p it can take small negative values. Furthermore, it converges to zero for $p \to 0$.

This behavior can be explained in the following way: Let us assume we have a message length $d = 2$. Since on average p nodes start a new transmission in each slot and they are chosen from the nodes that are idle, the nodes start to form two groups. One group of starts their transmissions in even slots; the other starts them in odd slots. This group formation is stronger for higher p. Hence, there is a negative correlation for even values of τ (as mostly the same nodes transmit in t and $t+\tau$) and positive correlation for odd values of τ (as mostly nodes of different groups transmit in these two slots).

For $d > \tau$ there are significantly higher correlation values for small p and in the limit for $p \to 0$ it approaches $\lim_{p\to 0}\rho(\tau) \overset{d\ge\tau}{=} \frac{d-\tau}{d}$. For higher p the correlation decreases and becomes negative.

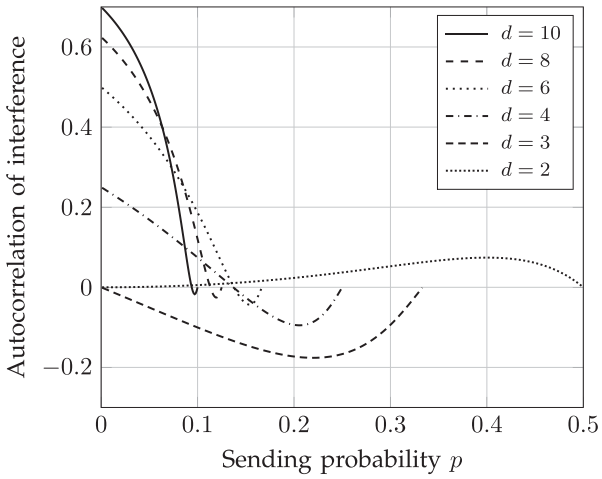

(a) The time lag is $\tau = 3$.

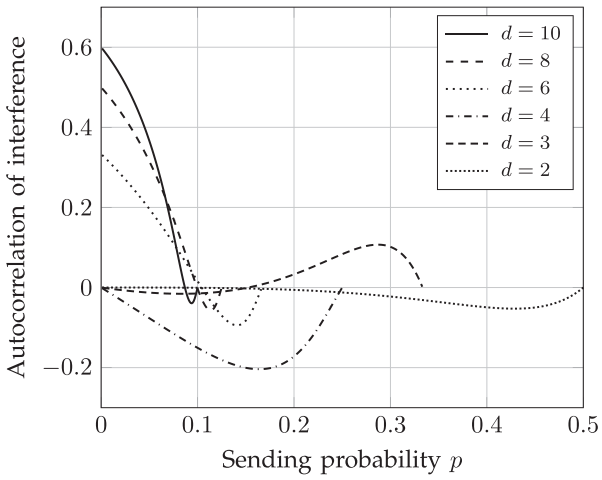

(b) The time lag is $\tau = 4$.

Fig. 8. Correlation for the case (0, 0, 2) for varying the sending probability p and message length d.

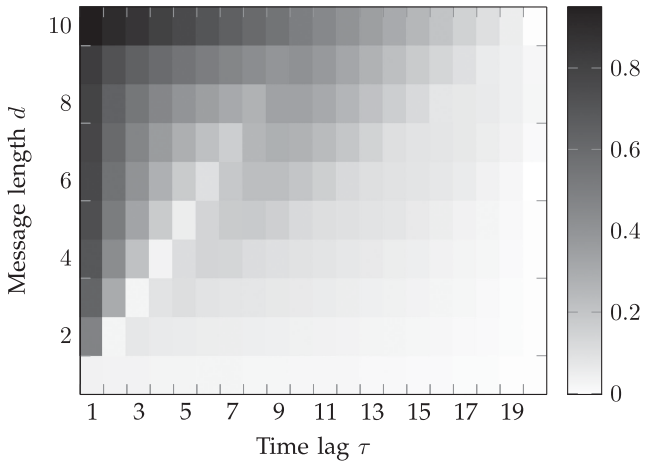

(a) Block fading model.

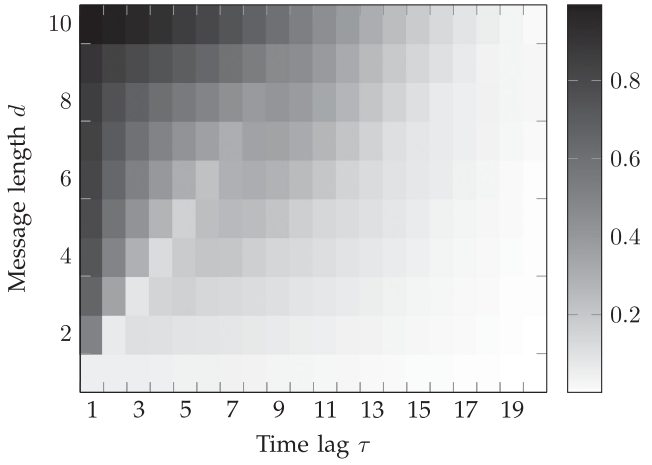

(b) Clarke's fading model.

Fig. 9. Correlation for the case (0, 2, 2) for varying message length d. The sending probability is $p = 0.1$, the channel coherence time is $c = 22$ for both fading models.

In all cases, we have $\lim_{p \to \frac{1}{d}} \rho(\tau) = 0$, which means that all nodes are always transmitting and hence there is zero variance and covariance.

5.4 Correlation by Multiple Sources

5.4.1 Channel and Traffic

Fig. 9 shows a heat map of the correlation when both channel and traffic introduce correlation (case (0, 2, 2)) for both fading models. Results are shown for $c = 22$. For given values of c and d, the correlation is highest for $\tau = 1$. For increasing τ, the correlation shows a damped oscillation around zero and vanishes in the limit $\tau \to \infty$. For each value of d, there is a sharp change of trend at two points: The first is at $\tau = c$ and the second at $\tau = d$. These are the points where the correlation caused by traffic and channel, respectively, are at their minimum. The contribution of the channel is zero for $\tau \geq c$, and the contribution of traffic is negative for $\tau = d$ and increases for further increasing τ.

The case $d = 10$ is special since all nodes are transmitting all the time (i.e., we have a traffic intensity $\mu = 1$). In such a setting, the traffic does not cause any correlation, and hence the correlation of interference is fully determined by the channel correlation. This corresponds to the case (0, 2, 0), in which the correlation has a linear dependence on τ (topmost row in the heat map).

When comparing Figs. 9a and 9b, almost no difference is noticeable, which indicates that the two fading models behave similar. In order to further investigate their similarity, we compare their correlation in Fig. 10. The comparison is performed assuming the same coherence time for both fading models, which can be achieved by inverting the expression for coherence time of Clarke's model (6). The results show that the exact correlation values are different, but the qualitative behavior is very similar. This justifies the use of the block fading model for interference analysis, as it is a good approximation of the mathematically more complex Clarke model.

5.4.2 Node Locations, Channel, and Traffic

When accounting for all three sources of interference correlation and no mobility (case (2, 2, 2)), the correlation evolves as shown in Fig. 11. Correlation starts at a high level for small τ and tends to decrease for increasing τ, although not monotonically, as there are also ranges of τ where correlation slightly increases. For τ beyond the message length d and channel coherence time c, the correlation approaches its static value as determined by the node locations (case (2, 0, 1)). In the limit

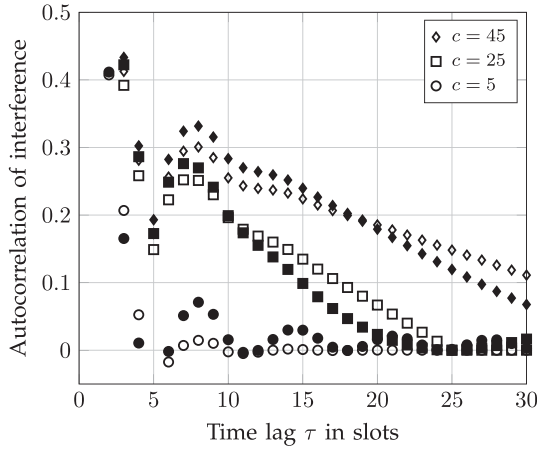

Fig. 10. Correlation for the case (0, 2, 2) for varying the channel block length c. Filled marks indicate Clarke's model; open marks indicate block fading. In both cases, we assume Rayleigh fading, the message length is $d = 5$, and the sending probability is $p = 0.1$.

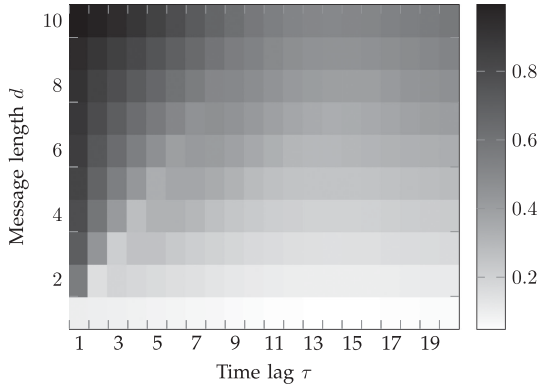

Fig. 11. Correlation for the case (2, 2, 2) for varying the message length d, the sending probability is $p = 0.1$, and the coherence time of Clarke's fading model is $c = 14$. A static network is considered ($v = 0$).

$\tau \to \infty$, it converges to the values of that case. This is explained by the fact that the contribution of the node locations to the interference correlation does not change with τ. Hence, for values of τ, for which the correlation contributions from other sources vanish, the node locations are the only source of correlation and fully determine its value.

The specific trends of the correlation are determined by the network parameters. The first qualitative change of the trend is the first local minimum, i.e., the point where it first starts to increase, which is located at $\tau = d$. This corresponds to case (0, 0, 2), where a similar local minimum is present. The second qualitative change of the trend can be found at $\tau = c = 14$, which is the time lag for which the correlation of the channel vanishes. The order of these two events depends on which of the parameters d and c has the higher value. Overall, the correlation behaves similar to case (0, 2, 2) with the difference that it approaches a nonzero constant value instead of zero correlation for high τ.

6 Coherence Time

Comparable to defining the channel coherence time (1), we define the *interference coherence time* to be the time lag until the correlation of the interference becomes small and hence the interference becomes stochastically independent from its original value.

Definition (Interference coherence time). *The interference coherence time τ_c is the minimum time lag τ such that the correlation is smaller than a threshold θ, i.e.,*

$$\tau_c = \min\{\tau \in \mathbb{N} \mid \rho(\tau) \leq \theta\}. \tag{35}$$

Remark. This is a subjective definition since τ_c is a function of θ, which has to be chosen in accordance to the considered case. The threshold below which interference can be assumed to be uncorrelated is in general greater than zero. If, for example, a scenario with no mobility and correlation from the node locations is considered (case $(2, j, k)$), correlation will not drop to zero, no matter how high the time lag τ.

The coherence time depends on the sources of correlation and the time they need to uncorrelate. In the following, we consider them separately to acquire an insight into their individual roles.

6.1 Impact of Traffic on Coherence Time

We consider the coherence time τ_c that results from a threshold $\theta = 0$. If all transmissions span d slots, the correlation of interference monotonically decreases for d slots (see Fig. 7). However, the coherence time is typically shorter, as the correlation is negative after d slots and hence crosses zero earlier, i.e., $\tau_c \leq d$. Thus, for the analysis of the coherence time we can adopt the simplified expression from Corollary 2.

In order to calculate the coherence time, we have to find the value of τ such that $\rho(\tau) = 0$. For general parameters there is usually no slot that exactly reaches zero correlation and therefore we instead calculate the time lag τ until correlation reaches zero and then round to the next higher integer.

Theorem 3 (Coherence time for case (0, 0, 2)). *The coherence time if traffic is the only source of correlation is*

$$\tau_c = \left\lceil \frac{\log(1-\mu)}{\log q} \right\rceil, \tag{36}$$

where $q = 1 - \frac{p}{1-p(d-1)}$ and ceiling function $\lceil x \rceil$.

Proof. The correlation of interference $\rho(\tau)$ is defined as in Theorem 2. Since traffic is the only source of correlation, we substitute $\mathbb{E}[h_{t_1}^2 h_{t_2}^2] = \mathbb{E}[h_t^4] = 1$. Further, we substitute the result of Corollary 2 for $\mathbb{E}[\gamma_{t_1} \gamma_{t_2}]$ into Theorem 2 yielding

$$\rho(\tau) = \frac{p(d-\tau) + p\,\frac{\tau(1-q)+q^{\tau+1}-q}{1-q} - \mu^2}{\mu - \mu^2}. \tag{37}$$

Solving the equation $\rho(\tau) = 0$ for the time lag τ gives

$$\tau = \frac{\log(1-\mu)}{\log q}. \tag{38}$$

In general the solution of τ in this expression is a noninteger. We round it to the next higher integer as the correlation is monotonically decreasing with τ and we aim for a correlation being smaller or equal to zero. □

Remark. Although Theorem 3 has been derived without fading, the same expression holds for fading with

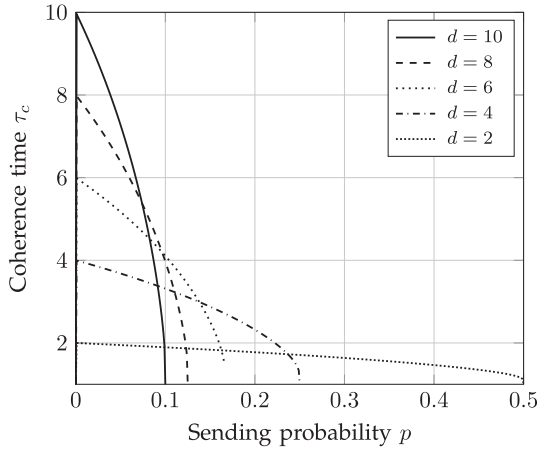

Fig. 12. Interference coherence time if considering solely the traffic as source of temporal correlation (case (0, 0, 2)) over the sending probability p for varying the message length d. In this plot, the rounding to the next higher integer is omitted to avoid high overlap of the curves, i.e., we plot (38) instead of (36).

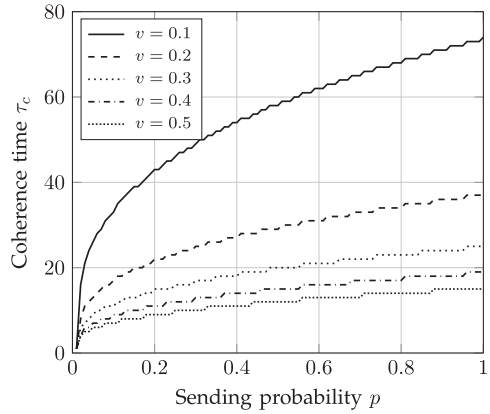

Fig. 13. Interference coherence time considering the node locations as sole source of temporal correlation (case (2, 0, 1)) with linear mobility. The results are plotted over the sending probability p for varying the velocity v, with $\theta = 0.01$. The steps in the plot occur since τ_c is measured in terms of slots and hence is integer.

$c = 1$, i.e., for case (0, 1, 2), as the only consequence of fading is to divide the correlation by a constant value $\frac{m+1}{m}$.

Fig. 12 shows the corresponding plot of the interference coherence time. For very small sending probabilities p (close to zero), the coherence time is roughly equal to the message length ($\tau_c \approx d$). For increasing values of p, the coherence time is monotonically decreasing and approaches its minimum for $\mu \to 1$, which is $\lim_{p \to \frac{1}{d}} \tau_c = 1$. In this case, interference is uncorrelated already in consecutive slots.

It is interesting that the coherence time depends on the sending probability p. Protocols that require two uncorrelated slots (e.g., a retransmission protocol) must adjust the retransmission back-off interval (= time lag) to the traffic load of the network. For higher traffic load, the back-off interval could be shortened based on this coherence time result, leading to a lower transmission delay. There might be other reasons that prevent the back-off interval from being too short, but still this example illustrates the benefit of having a good understanding of interference dynamics.

6.2 Impact of Channel on Coherence Time

If the channel is the sole source of correlation, we have the following result.

Theorem 4 (Coherence time for case (0, 2, 1)). *The interference coherence time τ_c equals the channel coherence time c if the channel is the sole source of correlation.*

Proof. From Theorem 2 we have

$$\rho(\tau) = \frac{p\big(\mathbb{E}[h_{t_1}^2 h_{t_2}^2] - 1\big)}{\frac{(m+1)}{m} - p}, \tag{39}$$

where $\mathbb{E}[h_{t_1}^2 h_{t_2}^2]$ is given in (23) for block fading and in (25) for Clarke's model. For block fading, in the case $\tau = c - 1$ we have $\rho(\tau) = \frac{p}{c(1+m-mp))}$, which is always positive for $p > 0$. As for $\tau \geq c$ the correlation vanishes, the coherence time is always equal to c. For Clarke's model, we get $\rho(\tau) = \frac{pJ_0^2(2\pi f_D \tau)}{2-p}$, where coherence time is defined as the first occurance of $\rho(\tau) < \theta$. Substituting (6) for τ yields

$$\rho(\tau) = \frac{pJ_0^2\left(2\pi f_D \frac{J_0^{-1}(\sqrt{\theta})}{2\pi f_D}\right)}{2-p} = \frac{p\,\theta^2}{2-p}. \tag{40}$$

As for $\theta = 0$ we have $\rho(\tau) = 0$, it follows $\tau_c = c$. □

6.3 Impact of Node Locations on Coherence Time

If the node locations are considered as a source of correlation, it is important to assume mobility. Otherwise the temporal correlation caused by node locations only node locations is constant for all $\tau \geq 1$ and never reaches θ. If other sources of correlation exist, the correlation converges to this constant for $\tau \to \infty$ (actually the convergence is fast for reasonable values of c and d). Specifically, if the static node locations are the only source of correlation, we have $\rho(\tau) = p$, independent of τ (see [8], [9]). In this case, it makes no sense to talk about a coherence time.

Let us assume that nodes move at a velocity $v > 0$. The temporal correlation of the interference is monotonically decreasing to its limit $\lim_{t \to \infty} \rho(\tau) = 0$. For finite time, however, it will get arbitrarily small but remain positive. Hence we choose a threshold $\theta > 0$ for our analysis.

There is no closed-form expression of the coherence time of interference τ_c when correlation is induced by the node locations. This is due to the rightmost integration in (9) that has no closed-form solution and therefore cannot be rearranged to give an expression for τ. Accounting to this, we numerically evaluate the coherence time τ_c. Fig. 13 shows τ_c with a threshold $\theta = 0.01$ for varying sending probability p and different velocities v. The general trend corresponds to intuition: First, τ_c increases with increasing p, as the temporal correlation of interference increases with p, making the threshold θ to be crossed later. For very small sending probabilities the coherence time is very small (in the limit we have $\lim_{p \to 0} \tau_c = 1$), and the interference in consecutive slots is uncorrelated. This behavior opposes the trend in case (0, 0, 2), where the coherence time decreases with increasing p (see Fig. 12). Second, a higher velocity v leads to a smaller

coherence time, the reason being that nodes with higher velocity reach the decorrelation distance earlier.

The general trends are the same with Brownian motion, but the coherence times are higher. This is because the distance between the initial and final positions of a typical node increases slower due to the back and forth movements. We omitted a plot of these results as they do not provide further insights.

7 Conclusions

This article investigated the temporal dynamics of interference by means of correlation and coherence time using methods from stochastic geometry. We provided a mathematical framework of general validity for the computation of interference correlation in Poisson networks and derived specific expressions for wireless channels with Nakagami block fading and Rayleigh fading according to Clarke's model.

The shape of the correlation over τ looks as follows: It decreases for small τ with a slope depending on the correlation sources and reaches zero (no correlation) in some cases. It follows a damped or overdamped oscillation around/to zero or another value. Negative correlation can occur if the channel or traffic are considered as correlation sources. If the node locations are the sole source, mobility helps to reduce interference correlation. Nakagami block fading and Clarke's model lead to qualitatively similar behavior for both interference correlation and coherence time.

Further research is needed to assess how the derived expressions can be harnessed in the design of communication techniques and protocols.

Acknowledgments

This work has been supported by the Austrian Science Fund (FWF) under grant P24480-N15 (Dynamics of Interference in Wireless Networks) and by the K-project DeSSnet. The K-project DeSSnet is funded within the context of COMET—Competence Centers for Excellent Technologies—by the Austrian Ministry for Transport, Innovation and Technology (BMVIT), the Federal Ministry for Digital and Economic Affairs (BMDW), and the federal states of Styria and Carinthia. The program is conducted by the Austrian Research Promotion Agency (FFG).

References

[1] B. Sklar, "Rayleigh fading channels in mobile digital communication systems. I. characterization," *IEEE Commun. Mag.*, vol. 35, no. 9, pp. 136–146, Sep. 1997.

[2] J. G. Andrews, T. Bai, M. N. Kulkarni, A. Alkhateeb, A. K. Gupta, and R. W. Heath, "Modeling and analyzing millimeter wave cellular systems," *IEEE Trans. Commun.*, vol. 65, no. 1, pp. 403–430, Jan. 2017.

[3] Q. Cui, X. Yu, Y. Wang, and M. Haenggi, "The SIR meta distribution in Poisson cellular networks with base station cooperation," *IEEE Trans. Commun.*, vol. 66, no. 3, pp. 1234–1249, Mar. 2018.

[4] M. Haenggi, *Stochastic Geometry for Wireless Networks*. Cambridge, U.K.: Cambridge Univ. Press, 2013.

[5] U. Schilcher, S. Toumpis, M. Haenggi, A. Crismani, G. Brandner, and C. Bettstetter, "Interference functionals in Poisson networks," *IEEE Trans. Inf. Theory*, vol. 62, no. 1, pp. 370–383, Jan. 2016.

[6] M. Haenggi and R. Smarandache, "Diversity polynomials for the analysis of temporal correlations in wireless networks," *IEEE Trans. Wireless Commun.*, vol. 12, no. 11, pp. 5940–5951, Nov. 2013.

[7] M. K. Atiq, U. Schilcher, J. F. Schmidt, and C. Bettstetter, "Semi-blind interferenece prediction in wireless networks," in *Proc. ACM Int. Conf. Model. Anal. Simul. Wireless Mobile Syst.*, Nov. 2017, pp. 19–23.

[8] R. Ganti and M. Haenggi, "Spatial and temporal correlation of the interference in ALOHA ad hoc networks," *IEEE Commun. Lett.*, vol. 13, no. 9, pp. 631–633, Sep. 2009.

[9] U. Schilcher, C. Bettstetter, and G. Brandner, "Temporal correlation of interference in wireless networks with Rayleigh block fading," *IEEE Trans. Mobile Comput.*, vol. 11, no. 12, pp. 2109–2120, Dec. 2012.

[10] M. Nakagami, "The m-distribution—a general formula of intensity distribution of rapid fading," in *Proc. Statistical Methods Radio Wave Propag.*, Jun. 1958, pp. 3–36.

[11] R. H. Clarke, "A statistical theory of mobile-radio reception," *Bell Syst. Tech. J.*, vol. 47, pp. 957–1000, Jul. 1968.

[12] Y. Zhong, W. Zhang, and M. Haenggi, "Managing interference correlation through random medium access," *IEEE Trans. Wireless Commun.*, vol. 13, no. 2, pp. 928–941, Feb. 2014.

[13] M. Haenggi, "Diversity loss due to interference correlation," *IEEE Commun. Lett.*, vol. 16, no. 10, pp. 1600–1603, Oct. 2012.

[14] U. Schilcher, C. Bettstetter, and G. Brandner, "Temporal correlation of interference: Cases with correlated traffic," in *Proc. ITG Conf. Syst., Commun. Coding*, Jan. 2013.

[15] R. Tanbourgi, H. S. Dhillon, J. G. Andrews, and F. K. Jondral, "Effect of spatial interference correlation on the performance of maximum ratio combining," *IEEE Trans. Wireless Commun.*, vol. 13, no. 6, pp. 3307–3316, Jun. 2014.

[16] R. Tanbourgi, H. S. Dhillon, J. G. Andrews, and F. K. Jondral, "Dual-branch MRC receivers under spatial interference correlation and nakagami fading," *IEEE Trans. Commun.*, vol. 62, no. 6, pp. 1830–1844, Jun. 2014.

[17] A. Crismani, S. Toumpis, U. Schilcher, G. Brandner, and C. Bettstetter, "Cooperative relaying under spatially and temporally correlated interference," *IEEE Trans. Veh. Technol.*, vol. 64, no. 10, pp. 4655–4669, Oct. 2015.

[18] M. Haenggi, J. G. Andrews, F. Baccelli, O. Dousse, and M. Franceschetti, "Stochastic geometry and random graphs for the analysis and design of wireless networks," *IEEE J. Sel. Areas Commun.*, vol. 27, no. 7, pp. 1029–1046, Sep. 2009.

[19] G. George, R. K. Mungara, A. Lozano, and M. Haenggi, "Ergodic spectral efficiency in MIMO cellular networks," *IEEE Trans. Wireless Commun.*, vol. 16, no. 5, pp. 2835–2849, May 2017.

[20] Z. Gong and M. Haenggi, "Interference and outage in mobile random networks: Expectation, distribution, and correlation," *IEEE Trans. Mobile Comput.*, vol. 13, no. 1, pp. 337–349, Feb. 2014.

[21] Z. Gong and M. Haenggi, "Temporal correlation of the interference in mobile random networks," in *Proc. IEEE Int. Conf. Commun.*, Jun. 2011, pp. 1–5.

[22] Y. Zhong, T. Q. S. Quek, and X. Ge, "Heterogeneous cellular networks with spatio-temporal traffic: Delay analysis and scheduling," *IEEE J. Sel. Areas Commun.*, vol. 35, no. 6, pp. 1373–1386, Jun. 2017.

[23] Y. Zhong, M. Haenggi, F. Zheng, W. Zhang, T. Q. S. Quek, and W. Nie, "Toward a tractable delay analysis in ultra-dense networks," *IEEE Commun. Mag.*, vol. 55, no. 12, pp. 103–109, Dec. 2017.

[24] C. Bettstetter, G. Resta, and P. Santi, "The node distribution of the random waypoint mobility model for wireless ad hoc networks," *IEEE Trans. Mobile Comput.*, vol. 2, no. 3, pp. 257–269, Jul. 2003.

[25] D. Tse and P. Viswanath, *Fundamentals of Wireless Communication*. Cambridge, U.K.: Cambridge Univ. Press, 2005.

[26] U. Schilcher, S. Toumpis, A. Crismani, G. Brandner, and C. Bettstetter, "How does interference dynamics influence packet delivery in cooperative relaying?," in *Proc. ACM/IEEE Int. Conf. Model. Anal. Simul. Wireless Mobile Syst.*, Nov. 2013, pp. 347–354.

Udo Schilcher received two Dipl.-Ing. degrees with distinction in computing and mathematics from the University of Klagenfurt, in 2005 and 2006, respectively. From 2005 to 2017, he was a research staff member at the Institute of Networked and Embedded Systems, University of Klagenfurt. His doctoral thesis was on inhomogeneous node distributions and interference correlation in wireless networks and he was awarded with a Dr. techn. degree with distinction in 2011. After his graduation, from 2011 he held senior positions in the Institute of Networked and Embedded Systems at the University of Klagenfurt and at Lakeside Labs GmbH. His main interests are interference dynamics and spatial node distributions in wireless networks, and stochastic geometry. He received a best paper award from the IEEE Vehicular Technology Society.

Jorge F. Schmidt received the BSc and DSc degrees in electrical engineering from the Universidad Nacional del Sur, Bahía Blanca, Argentina, in 2005 and 2011, respectively. From 2012 to 2014, he was a postdoctoral fellow with the Signal Processing and Communications Laboratory at the University of Vigo, Spain. In 2014, he joined the Institute of Networked and Embedded Systems group, University of Klagenfurt, Austria, where he is currently a senior researcher. Since 2016, he has also been a senior researcher at Lakeside Labs GmbH, Austria. His main research interests include the area of statistical signal processing and interference modeling and management for wireless communications systems. He received a best paper award from the ACM SIGSIM.

Mahin K. Atiq received the master's degree in information and communication engineering from Sejong University, Seoul, South Korea, in 2014. Since 2015, she has been a research and teaching staff member at the University of Klagenfurt with interests in wireless systems and stochastic modeling. She is working toward the doctoral degree in interference prediction in wireless networks.

Christian Bettstetter (S'98-M'04-SM'09) received the Dipl.-Ing. degree and the Dr.-Ing. degree (summa cum laude) in electrical and information engineering from Technische Universität München (TUM), Munich, Germany, in 1998 and 2004, respectively. He was a research and teaching staff member at the Institute of Communication Networks, TUM, until 2003. From 2003 to 2005, he was a senior researcher with DOCOMO Euro-Labs. He has been a professor at the University of Klagenfurt, Austria, since 2005, and founding director of the Institute of Networked and Embedded Systems since 2007. He is also the founding scientific director of Lakeside Labs, a research company on self-organizing networked systems. He is a senior member of the IEEE.